An *in-Vivo* Lateral Ankle Ligament Strain Behavior Assessment Technique for Potential Use in Robot-Assisted Therapy

Mingming Zhang, Yanxin Zhang, T Claire Davies, *and* Shane Xie, *IEEE Member*

***Abstract*— Ankle sprains are very common, especially in sports activities. Accurate assessment of ankle ligament strain behavior is crucial in understanding ankle function and optimizing ankle rehabilitation programs. This study proposed an *in-vivo* lateral ankle ligament strain assessment technique for potential use in robot-assisted therapy. It consists of two phases: real-time identification of ankle joint and subtalar joint orientations and simulation of lateral ankle ligament strain behavior. A healthy participant conducted robot-assisted rehabilitation exercises and the results compared to a kinematic model. The model was found to be realistic, leading to the conclusion that this method may be appropriate for determining lateral ankle ligament strain in robot-assisted therapy.**

I. Introduction

Ankle sprains are among the most frequent and typical musculoskeletal injuries of the lower extremities [1, 2]. From 2002 to 2006, a total of 82.971 ankle sprain were identified in the NEISS database and an estimated 2.15 ankle sprains occurred per 1000 person-years in the United States [3]. The frequently injured ligaments are the anterior talofibular ligament (ATFL), calcaneofibular ligament (CFL) and posterior talofibular ligament (PTFL) [1]. The effects of ankle ligaments in resisting excess forces remain unclear and rehabilitation of torn ligaments and reconstruction of unstable ankles would be enhanced by knowing more details of the function of sprained ankle ligaments [4]. Accurate assessment of ankle ligament strain behavior is crucial in understanding ankle function and optimizing ankle rehabilitation programs [5].

Various techniques have been used in assessing ligament strains in the past few decades. Colville, et al. [4] examined ankle ligament strains on cadavers. Beynnon, et al. [6] used the Hall effect transducer (implantable technique) to study anterior cruciate ligament strain behavior during rehabilitation exercises *in vivo*. Asla, et al. [7] used a combination of dual-orthogonal fluoroscopic and magnetic resonance imaging techniques for assessing ATFL and CFL but only in some static foot positions under non-weight-bearing conditions. These methods can not be applied in ankle ligament strain assessment in robot-assisted therapy. Wei, et al. [5] recently established a computational model for determining dynamic ankle ligament strain behavior during foot external rotation, but the use of image based techniques impedes the application in robot-assisted therapy. However, two reviews [8, 9] have been conducted by our group involving robot-assisted ankle rehabilitation and assessment respectively. It was found that few ankle rehabilitation robots have the function of real-time ankle assessment and few ankle assessment techniques could dynamically identify ankle ligament strain behavior in robot-assisted therapy.

This study proposes an *in-vivo* ankle ligament strain assessment technique for potential use in robot-assisted therapy. Lateral ankle ligaments are of primary interest.

II. Methodology

This assessment technique consists of two phases: real-time i) identification of ankle joint and subtalar joint orientations based on a biaxial ankle model and ii) simulation of ankle ligament strain behavior based on an OpenSim ankle model with four ligaments. The output of the first phase is the input to the second one while an ankle rehabilitation robot provides the input to the first phase.

A. Ankle rehabilitation robot

An updated ankle rehabilitation robot based on the one in [10] was used in this study, as shown in Fig. 1. One improvement was its stability with thicker fittings and welded joints. The pneumatic muscle actuators were offset for larger ROM of ankle adduction and abduction. Three angular potentiometers (91A1AB28B15L, Bourns Inc) were used for detecting angular positions of the footplate. Data were recorded in the form of text file from LabVIEW for offline processing, after data acquisition by the NI Compact RIO 9022 and NI 9205 module.

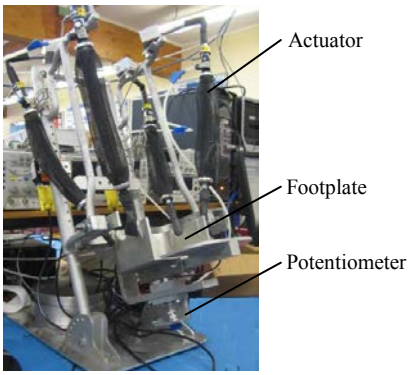

Figure 1. An updated ankle rehabilitation robot.

Resrach supported by the University of Auckland, Faculty of Engineering Research Development Fund-3625057 (Physical Robot-Human Interaction for Performance-Based Progressive Robot-Assisted Therapy).

M. Zhang, T C. Davies and S. Xie (Corresponding author) are with Department of Mechanical, University of Auckland, Auckland, New Zealand. (e-mails: mzha130@aucklanduni.ac.nz, c.davies@auckland.ac.nz, s.xie@auckland.ac.nz).

Y. Zhang is with Department of Sport and Exercise Science, University of Auckland. (e-mail: yanxin.zhang@auckland.ac.nz).

978-1-4244-7929-0/14/$26.00 ©2014 IEEE

B. Identification of ankle and subtalar joint orientations

Three measured angular positions of the end effector of the ankle rehabilitation robot can be used to identify ankle joint and subtalar joint orientations. This study used the biaxial ankle model with constant axis orientations, in which the ankle and subtalar joints were represented by two separate revolute hinges [11, 12].

Calculation of ankle joint and subtalar joint orientations used a similar method with the one described by Tsoi and Xie [13]. The ankle, subtalar and foot coordinate frames were defined with respect to a fixed global frame located on the tibia and fibula which are considered to be fixed during robot-assisted ankle rehabilitation exercises, as shown in Fig. 2. The black, blue, red and yellow coordinate frames respectively represent the fixed global frame xyz_o, ankle joint frame xyz_a, subtalar joint frame xyz_s and foot frame xyz_f. The dotted line, fine line and heavy line respectively represent x, y and z direction. The dotted lines in blue and red represent the ankle joint and the subtalar joint, respectively. The fixed black and yellow coordinate frames as well as the neutral foot position were defined with the same orientations as that in [13]. The orientation of the neutral blue frame with respect to the fixed black frame was obtained by applying consecutive rotations about axis y and z of the black frame, whereas the orientation of the neutral red frame was defined by rotations about axis y and z of the blue frame. Subscripts a, s and f are used to represent quantities related to the ankle, subtalar and foot coordinate frames.

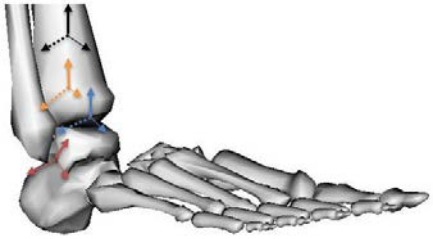

Figure 2. Coordinate frames of the foot-ankle complex. (dorsiflexion, adduction and inversion defined as positive whereas plantarflexion, abduction and eversion as negative [14])

Rotation matrices representing ankle, subtalar and foot coordinate frames at the neutral foot position with respect to the fixed global frame are given in (1) and (2). When the robot moves the foot to a certain position by applying rotations about ankle and subtalar joints, the foot orientation can be described in (3), where R_a^x and R_s^x represent the corresponding rotation matrices about the ankle joint and the subtalar joint. Equation (4) can be derived based on (1)-(3), where R_{oa} and R_{os} can be obtained based on anatomy from published literature [15, 16], R_{of} can be obtained based on measured results from the ankle rehabilitation robot.

$$R_{oa} = R_{oa}^{z} R_{oa}^{y} \tag{1}$$

$$R_{os} = R_{os}^{z} R_{os}^{y} \tag{2}$$

$$R_{of} = R_{oa} R_a^x R_{as} R_s^x R_{sf} \tag{3}$$

$$R_{of} = R_{oa} R_a^x R_{oa}^{-1} R_{os} R_s^x R_{os}^{-1} \tag{4}$$

Ankle and subtalar joint orientations during robot-assisted rehabilitation exercises can be identified by matching certain elements of the matrices defined in (5) and (6). To be specific, the ankle joint angle can be obtained by comparing A_{21} and B_{21}, A_{31} and B_{31}, and the subtalar joint angle can be obtained by comparing A_{12} and B_{12}, A_{13} and B_{13}.

$$A = R_{oa}^{-1} R_{of} R_{os} \tag{5}$$

$$B = R_{oa}^{-1} R_{os} \tag{6}$$

C. Lateral ankle ligaments modeling

Lateral ankle ligament modeling was based on the "bothlegs" in OpenSim [17]. Lateral talocalcaneal ligament (LTCL) is also included since subtalar instability is often associated with lateral ankle ligament injury [1]. Origins and insertion points of ATFL, CFL, PTFL and LTCL were defined based on recent published pictorial descriptions [18], as shown in Fig. 3. The coordinates of the origins and insertion points of these ligaments were obtained from the OpenSim model and summarized in Table I. All coordinates are represented in Tibia Frame (the origin locating on the top of tibia, the dotted line, the fine line and the heavy line representing x, y and z, respectively) defined by OpenSim to allow for efficient calculation. Ligament lengths and orientations were shown here and compared well with the published data from 42 lower limbs [19].

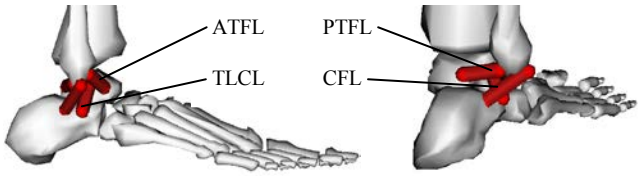

Figure 3. Lateral ankle ligaments (ATFL, CFL, PTFL and LTCL) in an OpenSim based model.

TABLE I. POSITIONS AND ORIENTATIONS OF LATERAL ANKLE LIGAMENTS

Ligament	Coordinate (mm)		Length (mm)	Orientation (°)		
	Origin	*Insertion Point*		*Sagittal Plane_XY*	*Transverse Plane_XZ*	*Frontal Plane_YZ*
ATFL	(3, 417, 31)	(15, -427, 15)	22.4	45.6876	26.5651	32.4563
CFL	(-3, -424, 41)	(-14, -443, 18)	31.8	46.3323	36.6950	20.2400
PTFL	(-7, -424, 25)	(-13, -428, 5)	21.3	70.1730	10.8445	16.3925
LTCL	(3, -427, 17)	(1, -443, 25)	18.3	25.8767	60.7941	12.6044

III. Experiments and Results

To validate this *in-vivo* lateral ankle ligament assessment technique, this study applied ligament strain with neutral length l_n as the reference as the assessment indicator. It was defined in (7), where l_t represents ligament length. The neutral state of the ligaments exists when the ankle joint and the subtalar joint are both in zero position defined in "bothlegs".

$$Strain = (\frac{l_t - l_n}{l_n}) * 100 \quad (7)$$

A. Participant

A healthy subject (Male, 28 years old, 172cm, 67kg) participated in this study. It was approved by the University of Auckland Human Participants Ethics Committee (9348). The right foot was fixed on footplate by Velcro straps and the intersection of the ankle joint and the subtalar joint was manually aligned with the rotation center of the footplate.

B. Experiments and Results

The participant was required to actively move his ankle in dorsiflexion/plantarflexion, inversion/eversion, and adduction/abduction. There is no any difference between active ankle motion and passive ankle motion for the developed ankle model. Data were recorded from LabVIEW with the sample being 100 Hz. Fig. 4 shows that the length of ATFL decreases with ankle dorsiflexion and increases with plantar flexion while those of CFL, PTFL and LTCL change oppositely.

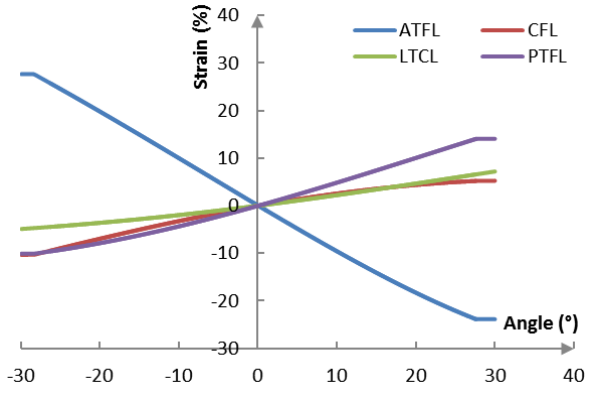

Figure 4. Lateral ankle ligament strain behavior in dorsiflexion/plantarflexion.

Fig. 5 describes the corresponding ligament strain behavior in inversion/eversion. The length of ATFL decreases with inversion and increases with eversion while those of CFL, PTFL and LTCL change oppositely. Fig. 6 shows that the length of PTFL decreases with adduction and increases with abduction while the opposite occurs for ATFL and LTCL. The length of CFL slightly increases with adduction and abduction.

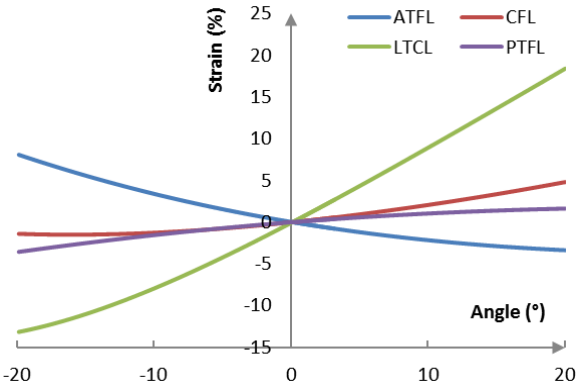

Figure 5. Lateral ankle ligament strain behavior in inversion/eversion.

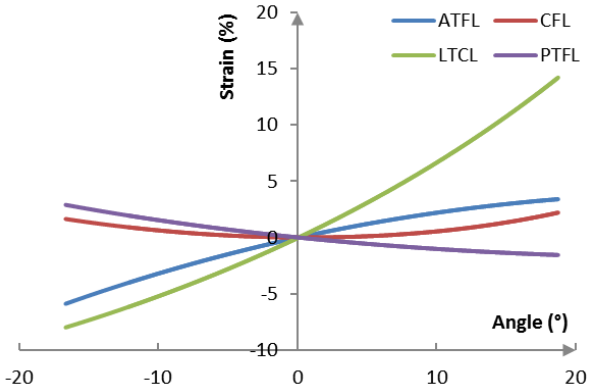

Figure 6. Lateral ankle ligament strain behavior in adduction/abduction.

IV. Discussion

For evaluation and rehabilitation of sprained ankle, it is generally accepted that disability level is divided into three grades based on how many ligaments get injured [1]. Our method aimed to assess lateral ankle ligament strain behavior in robot-assisted therapy that may be useful in identifying disability level of ankle sprains as rehabilitation progresses. Although marker based motion capture systems have been used for estimating joints kinematics and usually provide the input for musculoskeletal kinematics and kinetics analysis in OpenSim [17], such a motion system is not convenient to be used in robot-assisted rehabilitation exercises due to the issues of setup and time-consuming analysis. The proposed technique overcomes the limitation and has potential when combined with robot-assisted therapy due to the easy-collected input.

The strain of the ATFL, as shown in Fig. 4 increases with plantarflexion and decreases with dorsiflexion, which is in agreement with the data presented in [4, 7]. Opposite to the ATFL, the CFL strain increases with dorsiflexion and decreases with plantarflexion, corresponding to the experimental results. These data further validated the reciprocal function between ATFL and CFL [7]. Different elongations of ATFL and CFL for the same motion show that the former may get better rehabilitation in plantarflexion training whereas CFL is strengthened more effectively in

dorsiflexion training. Additionally, the PTFL length increases with dorsiflexion and decreases with plantar flexion, which is consistent with the published data presented in [4]. The CFL crosses the subtalar joint and thus its strain is sensitive to subtalar motion (Fig. 5). The CFL strain increases with inversion and decreases with eversion, which is also supported by the study of Colville, et al. [4]. The strain of LTCL is more obvious compared with that in CFL, to some extent which can account for that LTCL can be easily torn in severe ankle sprains [1]. Fig. 6 shows that the strain of LTCL is positive for ankle adduction, further demonstrating that the LTCL may get injured when the ankle is sprained. However, LTCL is usually considered as a variable structure, suggesting it can be contiguous with the inferior border of the ATFL and the CFL, or may be distinctly separate as it courses across the subtalar joint [20]. Thus, subject-specific LTCL origin and insertion points on the model are necessary. However, the assessment accuracy really depends on the used ankle model as well as the determination of the origins and insertion points of individual ligaments.

Limitations of this research should be noted. First, the identification of joint orientations and definition of origins and insertion points of all included ligaments were based on published data. Subject-specific data can be accurately obtained by image based methods. A second is the relative movement between the foot and the footplate, to some extent which minimizes the identification accuracy. This proposed model was developed based on a generic model, as the third limitation. However, furture research will focus on the development of the subject-specific model with ankle muscles and ligaments included. Evaluation in terms of ligament strain and passive joint torque will be conducted as well in near future.

V. Conclusion

A model based method for estimating individual lateral ankle ligament strain in robot-assisted therapy was proposed. The kinematic responses were found to be realistic, leading to the conclusion that this method is appropriate for lateral ankle ligament assessment in robot-assisted rehabilitation exercises. These evaluation results are usually required for the quantification of ankle sprain related disability level. They could provide the foundation for physiotherapists and robots to quantify ankle disability level and adjust rehabilitation strategies. They also help to understand the mechanism of how ankle ligaments are injured and how they can be best treated in rehabilitation.

Acknowledgment

This work was supported by the University of Auckland and China Sponsorship Council.

References

[1] G. J. Sammarco, *Rehabilitation of the Foot and Ankle*. Missouri, USA: Mosby-Year Book, 1995.

[2] D. T.-P. Fong, Y. Hong, L.-K. Chan, P. S.-H. Yung, and K.-M. Chan, "A Systematic Review on Ankle Injury and Ankle Sprain in Sports," *Sports Medicine* vol. 37, pp. 73-94 2007.

[3] B. R. Waterman, B. D. Owens, S. Davey, M. A. Zacchilli, and P. J. Belmont, "The epidemiology of ankle sprains in the United States," *Journal Of Bone And Joint Surgery-american Volume,* vol. 92, pp. 2279-84, Oct 6 2010.

[4] M. R. Colville, R. A. Marder, J. J. Boyle, and B. Zarins, "Strain measurement in lateral ankle ligaments," *The American Journal of Sports Medicine,* vol. 18, pp. 196-200, 1990.

[5] F. Wei, J. E. Braman, B. T. Weaver, and R. C. Haut, "Determination of dynamic ankle ligament strains from a computational model driven by motion analysis based kinematic data," *Journal of Biomechanics,* vol. 44, pp. 2636-2641, 2011.

[6] B. D. Beynnon, B. C. Fleming, R. J. Johnson, C. E. Nichols, P. A. Renström, and M. H. Pope, "Anterior Cruciate Ligament Strain Behavior During Rehabilitation Exercises In Vivo," *The American Journal of Sports Medicine,* vol. 23, pp. 24-34, 1995.

[7] R. J. d. Asla, M. Kozanek, L. Wan, H. E. Rubash, and G. Li, "Function of anterior talofibular and calcaneofibular ligaments during in-vivo motion of the ankle joint complex," *Journal of Orthopaedic Surgery and Research,* vol. 4:7, 2009.

[8] M. Zhang, T. C. Davies, and S. Xie, "Effectiveness of robot-assisted therapy on ankle rehabilitation -- a systematic review," *J Neuroeng Rehabil,* vol. 10, p. 30, Mar 21 2013.

[9] M. Zhang, T. C. Davies, Y. Zhang, and S. Xie, "Reviewing the effectiveness of ankle assessment techniques for use in robot-assisted therapy," *Journal of Rehabilitation Research & Development,* vol. 51, 2014.

[10] P. K. Jamwal, S. Q. Xie, S. Hussain, and J. G. Parsons, " An Adaptive Wearable Parallel Robot for Ankle Injury Treatments," *IEEE Transactions on Mechatronics,* vol. 19, pp. 64-75, 2014.

[11] J. Dul and G. E. Johnson, "A kinematic model of the human ankle," *Journal of Biomedical Engineering,* vol. 7, pp. 137-143, 1985.

[12] M. Dettwyler, A. Stacoff, I. A. Kramers-de Quervain, and E. Stüssi, "Modelling of the ankle joint complex. Reflections with regards to ankle prostheses," *Foot and Ankle Surgery,* vol. 10, pp. 109-119, 2004.

[13] Y. H. Tsoi and S. Q. Xie, "Online Estimation Algorithm for a Biaxial Ankle Kinematic Model With Configuration Dependent Joint Axes," *Journal of Biomechanical Engineering-Transactions of the Asme,* vol. 133, pp. 021005.1-021005.11, Feb 2011.

[14] G. Wu, S. Siegler, P. Allard, C. Kirtley, A. Leardini, D. Rosenbaum, M. Whittle, D. D. D'Lima, L. Cristofolini, H. Witte, O. Schmid, and I. Stokes, "ISB recommendation on definitions of joint coordinate system of various joints for the reporting of human joint motion—part I: ankle, hip, and spine," *Journal of Biomechanics,* vol. 35, pp. 543-548, 2002.

[15] G. S. Lewis, K. A. Kirby, and S. J. Piazza, "Determination of subtalar joint axis location by restriction of talocrural joint motion," *Gait & Posture,* vol. 25, pp. 63-69, 2007.

[16] R. E. Isman and V. T. Inman, "Anthropometric studies of the human foot and ankle," *Bull Prosth Res,* vol. 11, pp. 97-129, 1969.

[17] S. L. Delp, F. C. Anderson, A. S. Arnold, P. Loan, A. Habib, C. T. John, E. Guendelman, and D. Thelen, "OpenSim: Open-Source Software to Create and Analyze Dynamic Simulations of Movement," *IEEE Transactions on Biomedical Engineering,* vol. 54, pp. 1940-1950, 2007.

[18] P. Golano, J. Vega, P. A. de Leeuw, F. Malagelada, M. C. Manzanares, V. Gotzens, and C. N. van Dijk, "Anatomy of the ankle ligaments: a pictorial essay," *Knee Surgery, Sports Traumatology, Arthroscopy,* vol. 18, pp. 557-69, May 2010.

[19] F. Taser, Q. Shafiq, and N. A. Ebraheim, "Anatomy of lateral ankle ligaments and their relationship to bony landmarks," *Surgical And Radiologic Anatomy,* vol. 28, pp. 391-7, Aug 2006.

[20] M. Colville, "Surgical treatment of the unstable ankle," *Journal of the American Academy of Orthopaedic Surgeons,* vol. 6, pp. 368-377, 1998.